



Exploration of anticancer potential of hydroxamate derivatives as selective HDAC8 inhibitors using integrated structure and ligand based molecular modeling approach

Ekta Shirbhate^a, Divya^a, Preeti Patel^a, Vijay K Patel^a, Ravichandran Veerasamy^b & Harish Rajak^{*a}

^a Medicinal Chemistry Research Laboratory, Institute of Pharmaceutical Sciences,
Guru Ghasidas University, Bilaspur 495 009, India

^b Faculty of Pharmacy, AIMST University, Semeling, 08100 Bedong, Kedah Darul Aman, Malaysia
E-mail: harishdops@yahoo.co.in

Received 17 January 2020; accepted (revised) 11 November 2020

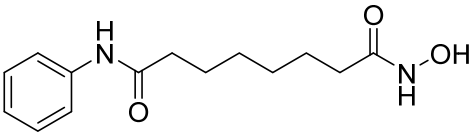
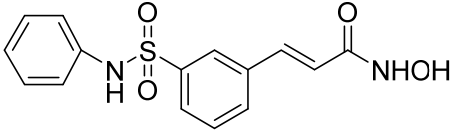
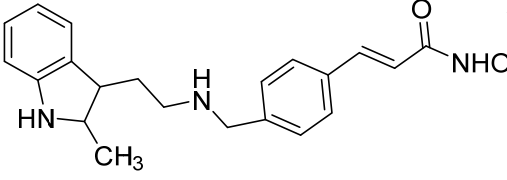
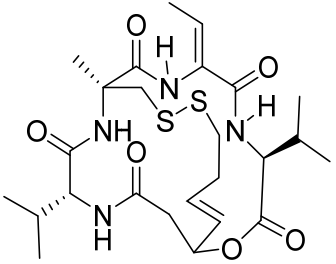
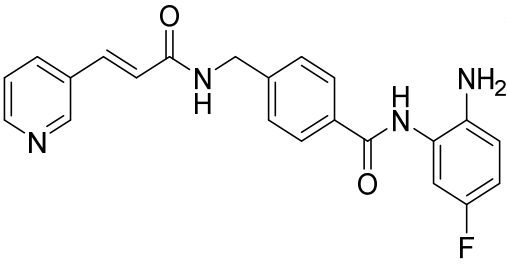
Recently, histone deacetylase inhibitors are evolving as an exhilarating new class of promising antitumor agents for the treatment of multiple malignancies. It may play a pivotal role as a therapeutic target for challenging the globally wide spread disease, cancer. At the same time, the prediction of biological activity of novel compounds, which was once a major challenge in drug design, is also pacing up its speed. This computational study has been performed in Schrodinger suite packages such as sitemap generation, grid formation, Glide for docking, Quikprop for ADME analysis, e-pharmacophore post docking script and Phase for 3D QSAR models designing, that all are available in Maestro version 9.3. Docking not only helps in predicting the preferred orientation of ligand with its target receptor, but also the binding affinity between the ligand and receptor. The application of Phase and e-pharmacophore script predicts some computational models of the provided ligands using 3D QSAR method. This decreases the cost and time of biological experiments. Glide XP reveals that compound **21** with the highest score value as the best compound from the dataset. Also, it shows good $R^2=0.9834$, $Q^2=0.7753$, stability = 0.5407 and low standard of deviation $SD=0.1085$ for hypothesis ADDRR.1601, for the PLS factor 5. The outcome of these studies suggests compound **21** as a potential drug molecule for HDAC targets.

Keywords: Structure-activity relationship; molecular docking; pharmacophore; 3D-QSAR; HDAC inhibitors

Cancer is now a serious disease that endangers human health. It is the second prominent root of death globally and is appraised to interpret for 9.6 million deaths in 2018 (as per WHO report). Lung, prostate, colorectal, stomach and liver cancer are recorded common types of cancer in men, though breast, colorectal, lung, cervix and thyroid cancer are the most common amongst women. In recent years, number of studies have shown that HDAC inhibitory drugs could inhibit the growth of tumors. There are many HDAC inhibitory drugs undergoing long research and development cycle¹⁻³. The steady process of histone acetylation is balanced by histone acetyltransferases (HATs) and histone deacetylases (HDACs). HATs makes the addition of acetyl groups to lysine residues of histone tails causing relaxation of chromatin and activation of transcription of nearby genes. On the contrast, HDACs remove the acetyl groups of acetylated histones leading to transcriptional suppression. HDAC therefore plays an important role in upregulating gene transcription, cell cycle progression and apoptosis. HDACs hence can be considered as a promising targets for cancer therapy⁴.

Till now, 18 mammalian HDACs have been identified and studied, which were divided into five groups: class I (HDAC1, 2, 3 and 8), class II which was further sub divided into class IIa (HDAC 4, 5, 7 and 9) and class IIb (HDAC 6 and 10), class III (SIRT 1 to 7) and finally class IV (HDAC 11)⁵⁻⁷. The enzymes of classes I, II and IV are Zn^{2+} dependent metallohydrolases^{5,7}. Class I enzymes are principally confined to the nucleus and are responsible for cell proliferation and differentiation^{5,8}. Class III enzymes are NAD^{2+} dependent Sir2-like deacetylases^{5,7}. Mainly, this class I and IIb are found to be over expressed in most hematological and solid tumors, extremely associating with a shoddiier prognosis. Consequently, class I and IIb target selective inhibitory agents turn out to be a key attention in cancer chemotherapy⁵. HDAC inhibitors are mainly recorded into few classes of hydroxamates, benzamides, aliphatic acids, cyclic tetra peptides, electrophilic ketones and some other types, suitably mentioned in table (Table I). This classification was based according to their chemical structures. At present, five HDAC inhibitors have been approved by FDA,

Table I — List of FDA approved HDAC inhibitors

Sr. No.	Class	List of HDAC inhibitors	Chemical structure	Year of approval	Approval agency	Targetting HDAC class	Application
1	hydroxamate	Vorinostat (SAHA)		2006	US-FDA	Pan	cutaneous T-cell lymphoma
2	hydroxamate	Belinostat (PXD-101)		2014	US-FDA	Pan	peripheral T-cell lymphoma
3	hydroxamate	Panabioistat (LBH-589)		2015	US-FDA	Pan	peripheral T-cell lymphoma
4	cyclic peptide	Romidepsin (FK228)		2009	US-FDA	selective inhibits Class I, II, III	cutaneous T-cell lymphoma
5	benzamide	Chidamide		2014	CFDA	selective inhibits Class I, II, III	multiple myeloma

which plays a significant role in the treatment of various melanomas, again mentioned in (Table I). These all HDAC inhibitory drugs share a similar pharmacophore skeleton consisting of following four key binding components: zinc binding group (ZBG), linker, connecting unit and cap moiety. Structural modification of HDAC inhibitors are mainly focused on the cap and linker realms to optimize activity and selectivity⁹.

As it is evident, the process of drug discovery and development is very challenging, puzzling, expensive and time consuming. But gradually it has been accelerated due to the incorporation of computational tools and methods in this field. Over the last decade,

the CADD (computer aided drug design), also known as *in silico* screening has come to be a prevailing technique in drug discovery and design, as it covers a wide range of computational approaches and new methodologies. It possesses combination of various advanced features enabling it to construct track for the synthesis and screening of designated compounds for improved therapeutics. *In silico* drug designing includes various steps like molecular docking, homology modelling, multi target searching and designing, pharmacophore development, conformation generation and quantitative structure activity relationship (QSAR)¹⁰.

Result and Discussion

Molecular docking study

The results of molecular XP docking highlight apparent binding efficiency of hydroxamic acid based molecules with receptor protein 1T69 (Figure 1a). The compound **21** from the dataset showed maximum structural alignment with that of SAHA in protein 1T69. The interactions were metal coordination, hydrogen bonding (backbone and side chain), hydrophobic interaction, hydrophilic interaction and pi-pi stacking. The 2D interaction diagram (Figure 1b) of compound **21** docked with protein showed metallic bond interaction between keto group of molecule with Zinc (Zn378) of receptor 1T69. The 2D interaction diagram displayed hydrophobic interaction between PHE207 amino acid with five membered triazole ring, and PHE208 with terminal benzene ring. It displayed hydrophilic interaction of amino acid HIE180 with triazole moiety and HIS143 with triazole attached benzene ring of phenylhydroxylamine. Also, hydrogen bonding was noticeable at multiple positions: PHE152 and NH- group of hydroxamic acid scaffold, GLY206 and hydroxyl group of cap, TYR306 and keto group of connecting unit and finally between GLY151 and NH- moiety of connecting unit.

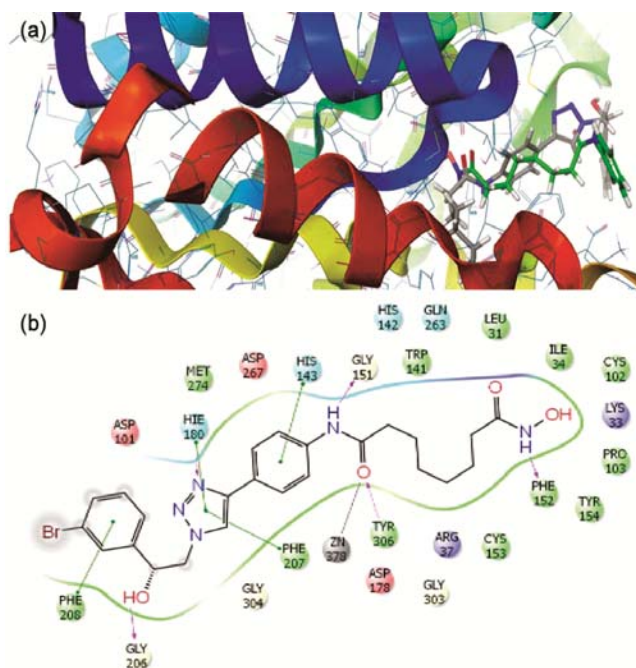


Figure 1 — Docking pose of compound **21** complexing with 1T69 protein (a) Docking pose alignment showing crystal ligand SAHA (green) and docked ligand (grey) (b) 2D interaction pattern of ligand with protein

ADMET analysis

It utilizes the physicochemical parameters to explain the vital properties affecting the biological functions. Permeability, solubility, lipophilicity, integrity, stability, *etc.* are some important measurable physicochemical properties. Though the concept of ADME has now been extended to toxicity. Right from the starting of drug discovery, the *in silico* method is helpful in predicting pharmacokinetic properties for instant ADMET. Among the dataset of 38 compounds, 10 compounds were filtered through Quikprop feature (Table II).

Energetic (e)- Pharmacophore study

The result of e-pharmacophore hypothesis study displayed hypothesis for compound **21** with protein 1T69. As default, maximum of seven pharmacophoric features were adopted. The generated hypothesis represented one hydrogen bond acceptor, three hydrogen bond donors, two aromatic rings and one hydrophobic/ non polar group (Figure 2a). Its ranking order and scoring value specify that the aromatic rings, R14 and R15 creates hydrophobic environment. The acceptor, A6 and donor, D8, D9 and D10 participates in hydrogen bonding. Ultimately, non-polar group, H12 involved in hydrophobic enclosure interaction. (Table III)

Pharmacophore modelling

The result for pharmacophore and atom centered 3D QSAR modelling was attained from “Phase” v3.4 feature of Maestro. The best 10 hypotheses were selected (Table IV) and thereby on relating the survival score of all the spawned hypotheses, it directed that pharmacophore model generated by hypothesis ADDR.1601 has the preeminent survival score (Figure 2b). It disclosed the best alignment over most active molecule accompanying distance (Å). The ligand based pharmacophoric model, ADDR.1601 unveiled five significant features counting one hydrogen bond acceptor, two hydrogen bond donors and two aromatic rings showing highest survival score value of 3.178.

3D-QSAR Modelling

The prime aim of developing 3D-QSAR model is to facilitate a mathematical relationship between the 3D spatial layout of the pharmacophoric features with the cytotoxic activity of HDAC inhibitory drugs. The

Table II — Analysis of physicochemical properties and biological functions of filtered molecules from the dataset of 38 compounds by using Quikprop

Compd. No.	Mol. Weight (g/mL) (130.0 to 725.0)	Volume (500.0 to 2000.0)	SASA (300 to 1000)	Acceptor H bond groups (2.0 to 20.0)	Donor H bond groups (0.0 to 6.0)	Number of Ring atoms	QPlogPw (4.0 to 45.0)	Human oral absorption (1, 2, 3 for low, medium, high)	CNS (-2 for inactive, +2 for active)	Rule of five (Number of violations of Lipinski's rule of five)
1	466.499	1532.17	885.656	12.95	3	12	22.182	1	-2	1
3	546.544	1732.322	1000.43	16.2	4	17	28.437	1	-2	2
8	559.586	1800.025	1028.035	16.2	4	17	27.954	1	-2	1
9	440.464	1451.384	839.528	13.7	3	11	22.741	1	-2	1
12	533.368	1441.492	839.461	8.7	3	17	18.947	2	-2	1
21	530.42	1569.961	902.493	10.9	4	17	22.04	2	-2	1
25	530.42	1570.055	902.637	10.9	4	17	22.037	2	-2	1
29	530.42	1553.052	880.96	10.4	4	17	21.42	2	-2	1
33	530.42	1548.908	882.869	10.4	4	17	21.414	2	-2	1
38	466.499	1553.764	908.892	12.95	3	12	22.483	1	-2	1

SASA = total Solvent Assessable Surface Area in square angstroms using a probe with a 1.4Å radius. QPlogPw = predicted water/gas partition coefficient.

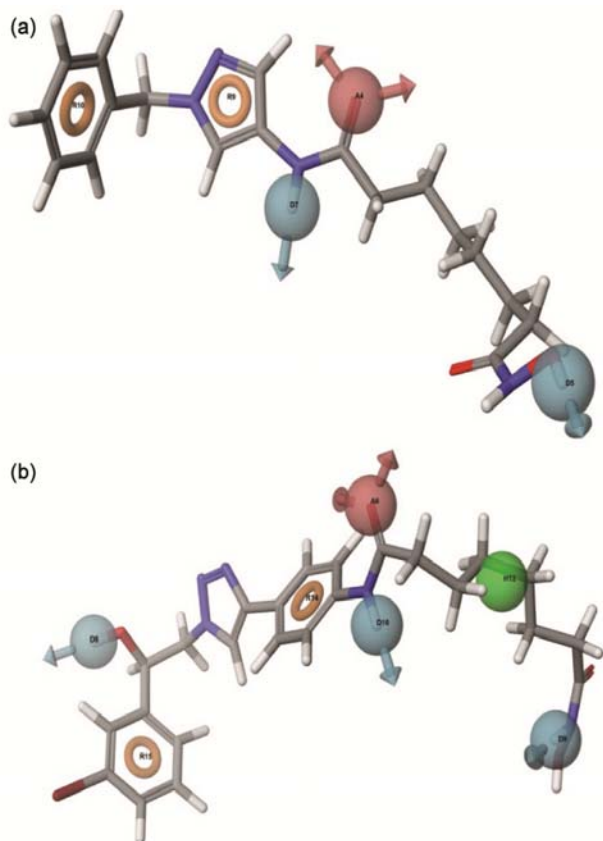


Figure 2 — Pharmacophore hypothesis. Pharmacophore features elucidating hydrogen bond acceptor (A, pink), hydrogen bond donor (D, blue) and aromatic rings (R, brown) (a) Pharmacophore model ADDDHRR developed using the e-pharmacophore script (ligand and structure based approaches) (b) Pharmacophore model AADRR.1601, developed using the Phase module (ligand based approach)

Table III — Score of pharmacophoric features based on energetic terms of XP docking

Rank	Feature label	Score (kcal / mol)	Score source
1	R14	-1.89	Ring ChemscoreHPhobe
2	D8	-0.59	H Bond
3	D9	-0.59	H Bond
4	D10	-0.59	H Bond
5	H12	-0.55	PhobEn + none
6	A6	-0.35	H Bond
7	R15	-0.62	Ring ChemscoreHPhobe

data set of 38 compounds were distributed into active, moderately active and inactive array, based on assumed activity threshold (6.80-5.80). A total of 38 molecules were additionally partitioned into training set (27) and test set (11). Five featured containing CPH (ADRR.1601) was selected for atom-based 3D QSAR model development, considering PLS factor as 5. The CPH ADRR.1601 executed best statistical conclusion for PLS factor 5 revealing Q^2 (0.7753), R^2 (0.9834), SD (0.1085), F (261), P (8.185e-019), RMSE (0.265), stability (0.5407) and Pearson-R (0.7478) (Table V). The predicted activities of training and test set, along with their fitness value for CPH ADRR.1601 is represented in Table IV. The residual values were computed by reduction of predicted activity from observed activity. The sum of residual value was computed as -0.1684 for model generated from hypothesis ADRR.1601 (Table VI). Scatter plots of actual vs. predicted activity for both training and test

Table IV — Hypothesis Score generated by Phase

Sr. No.	Hypothesis	Survival	Survival-inactive	Post-hoc	Site	Vector	Volume	Matches
1	ADDRR.1601	3.282	1.06	3.282	0.75	0.956	0.573	5
2	AADDR.2385	3.237	1.166	3.237	0.76	0.952	0.516	5
3	AAAHR.301	3.178	1.52	3.178	0.652	0.878	0.652	5
4	ADDHR.2499	3.352	1.856	3.352	0.75	0.912	0.665	5
5	AAHRR.1891	3.145	1.336	3.145	0.67	0.875	0.6	5
6	AADHR.1245	3.35	1.3	3.35	0.76	0.989	0.596	5
7	ADHRR.127	3.228	1.855	3.228	0.66	0.93	0.643	5
8	DDHRR.217	3.333	1.628	3.333	0.72	0.942	0.668	5
9	AAAHR.2654	3.339	2.093	3.339	0.67	0.958	0.706	5
10	AADDH.6219	3.347	1.926	3.347	0.82	0.93	0.598	5

Table V — Statistical result of the developed 3D QSAR model using ADDR.1601 CPH

ID	PLS fact.	SD	R ²	F	P	Stability	RMSE	Q ²	Pearson-R
ADDRR.1601	1	0.3674	0.7756	89.9	6.375e-010	0.8254	0.3432	0.6292	0.7652
	2	0.2169	0.9248	153.6	9.034e-015	0.6855	0.2836	0.7446	0.8201
	3	0.1473	0.9667	232.2	7.397e-018	0.5863	0.3003	0.6964	0.8585
	4	0.1270	0.9763	236.7	2.509e-018	0.5662	0.2825	0.7300	0.8632
	5	0.1085	0.9834	261	8.185e-019	0.5407	0.2650	0.7753	0.8779

Table VI — Comparison between experimental and predicted activity along with fitness values of dataset ligands, which are obtained from the best generated atombase3D-QSAR models ADDR.1601

Lig. Name	QSAR set	Experimental activity	3D QSAR ADDR.1601			Pharma Set
			Predicted activity	Residual	Fitness	
1	training	5.134	5.10	0.034	2.54	Inactive
2	test	6.151	6.12	0.031	1.88	+
3	test	6.186	6.01	0.176	1.34	+
4	training	7.119	7.18	-0.061	2.80	Active
5	training	7.086	7.12	-0.034	2.26	Active
6	training	7.553	7.49	0.063	2.22	Active
7	training	6.833	6.85	-0.017	1.94	Active
8	training	6.321	6.35	-0.029	2.35	+
9	training	7.770	7.81	-0.04	1.84	Active
10	training	5.556	5.24	0.316	2.01	Inactive
11	training	4.921	5.04	-0.119	2.00	Inactive
12	training	4.523	4.85	-0.327	2.00	Inactive
13	training	5.282	5.26	0.022	1.86	Inactive
14	training	5.879	5.92	-0.041	1.79	Inactive
15	test	5.924	5.78	0.144	2.86	+
16	training	5.379	5.37	0.009	1.81	Inactive
17	training	5.561	5.52	0.041	2.03	Inactive
18	test	5.401	5.80	-0.399	1.64	Inactive
19	training	6.099	6.11	-0.011	1.64	+
20	test	5.706	5.77	-0.064	1.57	Inactive
21	training	5.504	5.50	0.004	3.00	Inactive
22	test	5.701	6.13	-0.429	2.81	Inactive
23	training	6.258	6.33	-0.072	1.80	+
24	training	5.556	5.55	0.006	1.99	Inactive
25	training	6.357	6.37	-0.013	1.92	+
26	training	6.102	6.06	0.042	2.60	+

(contd.)

Table VI — Comparison between experimental and predicted activity along with fitness values of dataset ligands, which are obtained from the best generated atombase3D-QSAR models ADDRR.1601 (*contd.*)

Lig. Name	QSAR set	Experimental activity	Predicted activity	Residual	Fitness	Pharma Set
3D QSAR ADDRR.1601						
27	training	5.697	5.65	0.047	1.62	Inactive
28	test	6.286	6.01	0.276	1.97	+
29	training	6.133	6.09	0.043	1.58	+
30	test	6.634	6.37	0.264	2.06	+
31	training	6.277	6.27	0.007	1.94	+
32	training	6.026	5.95	0.076	1.92	+
33	test	6.391	6.04	0.351	1.73	+
34	test	5.745	5.90	-0.155	1.54	Inactive
35	training	5.398	5.36	0.038	0.87	Inactive
36	training	5.721	5.74	-0.019	1.53	Inactive
37	training	5.567	5.54	0.027	1.85	Inactive
38	test	5.134	5.52	-0.386	0.32	Inactive

+ Represents moderately active compounds.

set molecules were contrived (Figure 3). It could be used to sketch the actuality of QSAR model.

Model visualization

The 3D QSAR models were established for the dataset of compounds using common pharmacophore hypothesis ADDRR.1601, for validation purpose. An expressive demonstration of the cubes produced in 3D QSAR model (Figure 4), illuminating features like hydrogen bond donor, hydrophobic / non-polarity and electron withdrawing nature. The pink colored cubes reveal favorable condition, while the yellow cubes showing unfavorable condition for biological activity. The ligand 4 from the dataset which was more specifically from the training set was selected as the template molecule for building model with CPH ADDRR.1601. It enables much better understanding of the study.

The replacement of H attached with nitrogen atom of hydroxamate moiety with hydrogen donating group shows an increase in activity, however in contrary, hydroxyl group of this hydroxamate moiety when replaced by H donating groups exhibit antagonistic effect and hence it may be replaced with some other H-bond acceptors for an improvement in activity. Also the methylene attached directly with ZBG showing favorable nature for activity, displaying that on increasing unsaturation at this position may lead to decrement or loss in activity. The model also reveals any kind of substitution of hydrophobic group at various positions on benzene ring is helpful for activity. Similarly, replacing H of methylene group that is present in between benzene and pyrazoyl with non-polar atom

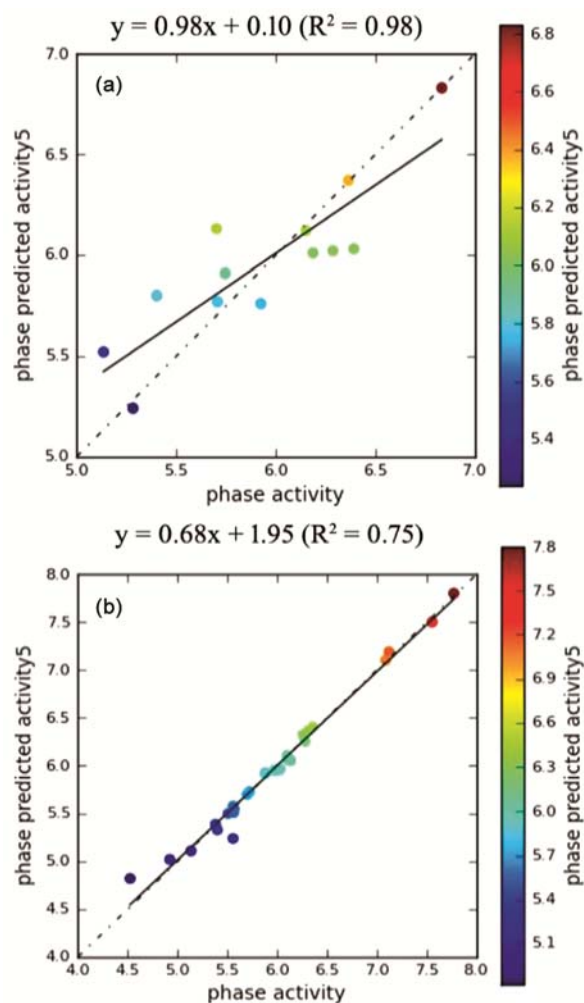


Figure 3 — Training (a) and test (b): Plots showing observed activity *versus* predicted activity, for 3D QSAR models generated using ADDRR.1601

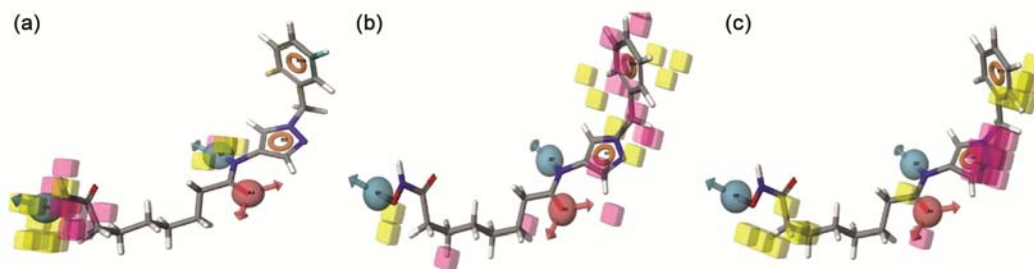


Figure 4 — Visualization of QSAR models generated using hypotheses ADDRR.1601 for various substituent groups (a) H-bond donor (b) Hydrophobic / non polar (c) Electron withdrawing. Pink cubes indicate favorable regions, whereas Yellow cubes indicates unfavorable regions for the activity.

would favour for activity and oxygen of hydroxyl part of ZBG would decrease its activity. In addition, substitution of electron withdrawing group in pyrazole ring and *ortho* and *meta* position of benzene ring leads to rise and fall in activity, respectively. Also, again it shows that on replacing H of methylene moiety adjacent to ZBG may result in decrement in activity.

The conclusion of this computational task evidently reveal that compound **21** is achieving many traits of high docking score, good ADME properties with lower toxicity, highest fitness value, better drug physicochemical properties and desirable conformation than the original ligand. Hence it can be considered as a potential lead molecule.

Material and methods

This computational tasks like protein preparation, ligand preparation, grid development, Glide XP molecular docking, ADME analysis, e-pharmacophore script generation and 3D QSAR model designing were performed out by employing various features of Schrodinger suite (Maestro version 9.3) LLC, New York software¹¹.

Dataset preparation

The dataset of 38 compounds possessing hydroxamic acid as preeminent scaffold, although showing wide structural variance, were selected from acceptable research papers for computational analysis. The compounds were found to exhibit same biological assay *i.e.*, fluorescence assay method¹². Molecular structures and activity information of compounds engaged for 3D QSAR study (Table VII). The IC_{50} values were converted into negative logarithm of IC_{50} (pIC_{50})¹³. The IC_{50} value was used as a dependent variable in QSAR study. These data are important for observing structure activity relationship by establishing effective 3D QSAR models.

Protein preparation

The protein was endowed by the “protein preparation wizard” tool in Maestro v9.3 (Schrodinger, LLC, NY). Primarily, it was essential to identify the binding region and binding mode of HDAC inhibitor, that was done by complexing crystal structure of SAHA with HDAC protein (PDB ID: 1T69)¹⁴. The work was accomplished in three steps, (i) Import and process: drifting the protein from recognized database (PDB) and processing it to fix its structure; (ii) Review and modify: deleting unwanted changes and solving some protein problems such as missing side chain and backbone and also, updating the missing residues. The water molecules occupying target creates difficulty in docking simulation and hence evacuated¹³. (iii) Refine: optimizing the orientation of H-bonding groups and minimizing the structure by OPLS_2009 force field^{14,15}.

Ligand preparation

The dataset of ligands were constructed and processed through “Lig prep” v2.5 tab in Maestro v9.3 (Schrodinger, LLC, NY). The molecular structures of these ligands were traced in Chemdraw Professional v16.0 and retained in mol format. The molecules were converted from 1D (Smiles) and 2D (SDF) representation to 3D structures, probed for tautomers and steric isomers and geometric minimization of ligands through OPLS_2005 force field. The partial atomic charges were enumerated by OPLS_2005 (Optimized Potential Liquid Simulation) force field^{11,16}.

Binding site analysis and grid generation

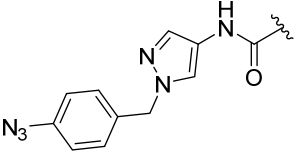
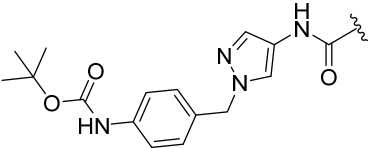
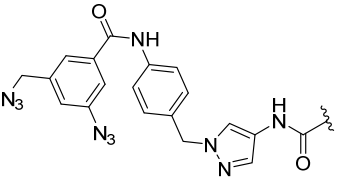
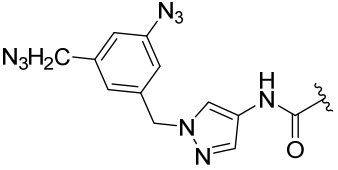
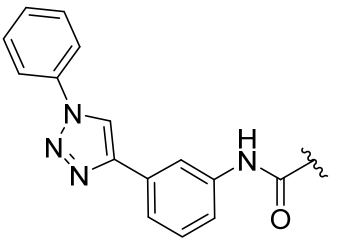
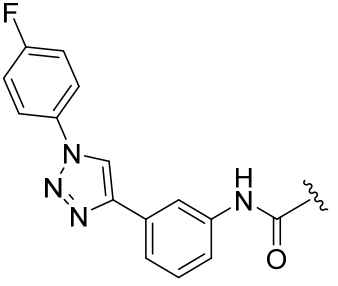
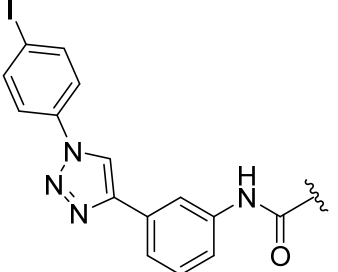
The site analysis plays a pivotal role in molecular docking research analysis. It efficiently exposes the active site in the target protein welcoming the impressive binding of drug. This assessment was

Table VII — Chemical structures and pIC₅₀ values of the selected compounds for the dataset

Sr.No.R	HDAC8 (μM)	IC ₅₀ pIC ₅₀ Sr.No.R	HDAC8 (μM)	IC ₅₀ pIC ₅₀
1	7.340	5.13420	1.970	5.706
2	0.707	6.15121	3.130	5.504
3	0.651	6.18622	1.990	5.701
4	0.076	7.11923	0.552	6.258
5	0.082	7.08624	2.780	5.556

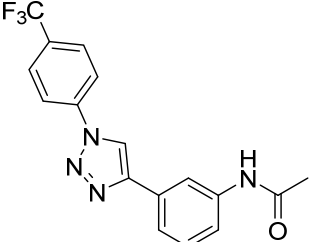
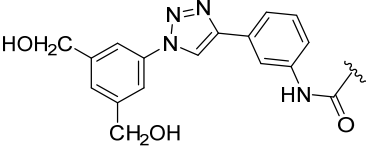
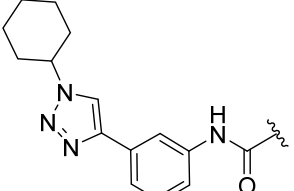
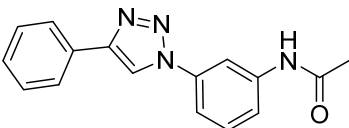
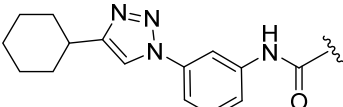
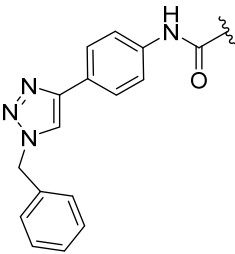
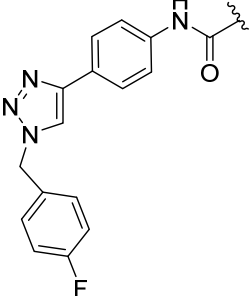
(contd.)

Table VII — Chemical structures and pIC₅₀ values of the selected compounds for the dataset (contd.)

Sr.No.R	HDAC8 (μ M)	IC ₅₀ pIC ₅₀ Sr.No.R	HDAC8 (μ M)	IC ₅₀ pIC ₅₀
6	0.028	7.55325		0.440 6.357
7	0.147	6.83326		0.790 6.102
8	0.487	6.32127		2.010 5.697
9	0.017	7.77028		0.518 6.286
10	2.780	5.55629		0.737 6.133
11	12.000	4.92130		0.433 6.364
12	30.000	4.52331		0.529 6.277

(contd.)

Table VII — Chemical structures and pIC₅₀ values of the selected compounds for the dataset (*contd.*)

Sr.No.R	HDAC8 (μM)	IC ₅₀ pIC ₅₀	Sr.No.R	HDAC8 (μM)	IC ₅₀ pIC ₅₀
13	5.220	5.28232		0.942	6.026
14	1.320	5.87933		0.406	6.391
15	1.190	5.92434		1.8	5.745
16	4.180	5.37935		4.0	5.398
17	2.750	5.56136		1.9	5.721
18	3.970	5.40137		2.71	5.567
19	0.797	6.09938		7.34	5.134

entirely considered along the surface and interior regions of the target by the sitemap generation course. In target 1T69 protein, suberoylanilide hydroxamic acid (SAHA) was selected as the suitable active site for grid generation¹¹. The “receptor grid generation” panel of Glide tab analyzes and work by fixing the drug target site in the target molecule. The receptor grid box was generated in a cubical shape having X: 20Å; Y: 20Å; Z: 20Å coordinates. The default values of Vander Waals’ radii scaling factor, charge scaling factor and partial charge cutoff were 1.0, 1.0 and 0.25, respectively¹⁴. The grid generated helps to finalize the ligand docking method¹¹.

Molecular docking (XP Docking)

In this research, “Glide” v5.8 (Schrodinger, LLC, NY), a molecular docking tool was used for docking studies to predict ligand efficiency, binding affinity and inhibitory constant towards target. The dataset of ligands was docked with the active of target using Glide extra precision approach¹¹ providing XP docking score. It provides a peculiar scoring function in form of GScore values¹⁴ that helps in identifying the best possible conformer with the most favorable binding affinity^{14,17}. The GScore comprises of the summation of XP terms obtained from hydrophobic grid potential and segment of the total protein ligand, π - π stacking, π -cation interaction, Vanderwaal energy, various rewards (*i.e.*, electrostatic ligands with low molecular weight), various penalties (*i.e.*, intra-ligand contacts, rotatable bond) and other interactions.

ADMET analysis

The Quikprop tool in Maestro v9.3 provides information about ADMET properties of compounds. Some of these properties includes H-bond donor group, H-bond acceptor group, SASA, Blood-Brain Barrier (BBB), QPlogPw, human oral absorption, rule of five and CNS¹¹.

Energetic (e)-Pharmacophore hypothesis generation

The e-pharmacophore hypothesis generation employs an integrated structure and ligand based method. It was performed through “docking post processing” option under e-pharmacophore script tab in Maestro v9.3 application¹⁴. The energetic values of XP Glide scoring function was used to map energy optimized pharmacophore (e-pharmacophores). Consequently, pharmacophore sites were created by employing “Phase” tool with six default chemical

features: hydrogen bond donor (D), hydrogen bond acceptor (A), hydrophobic/non-polar group(H), negative ionisable (P), positive ionisable (N) and aromatic ring (R). Each pharmacophore site generated comprises of cumulated values of XP Glide docking energies of the atoms. Sites were then graded according to their docking energies and the most justified site was screened for hypothesis¹⁷.

Pharmacophore modelling

The “Phase v3.4” tool in Maestro v9.3 helps to develop ligand-based pharmacophore models which impressively guide for common pharmacophore identification and 3D QSAR model formation. The exercise was started with the cleaning of all 38 ligands. The ligands were then subjected to conformer generation macromodel search method to generate their conformers keeping maximum number of conformers as 1000 per structure and these structures were then minimized employing OPLS 2005 force field using 100 minimization steps^{12,18,24}. The sites generated for ligands provide different pharmacophore hypotheses on the basis of activity threshold of active and inactive molecules. Each pharmacophore hypothesis contains a maximum of six chemical features: hydrogen bond donor (D), hydrogen bond acceptor (A), hydrophobic/non-polar group(H), negative ionisable (P), positive ionisable (N) and aromatic ring (R). These generated hypotheses were graded based on their survival, survival inactive, post-hoc scores, vector, volume and site scores^{12,19,24}. The best pharmacophore model was screened and identified by suitable aligning of the active ligand with hypothesis providing additional useful information for the further QSAR studies^{12,20}.

Atom based 3D QSAR modelling

The atom based 3D QSAR model designing was done using best fit designated hypothesis possessing the good scoring value. The dataset was efficiently divided into training and test set for analysis. The distribution was done such that 80% of the molecules fall within the training set and the remaining 20% as the test set fluctuating from maximally active to moderate and then smallest active (on the basis of IC₅₀) compounds^{12,21}. The activity threshold was assumed between 6.8 to 5.8. The grid spacing was maintained as 1Å and 5 as maximum PLS factor^{12,22}. The model designed must show good statistics and predictive ability. The QSAR result was finally

visualized to optimize the core structure of molecule^{12,18,22,23,24}.

Conclusion

The present research work highlights the strategy of innovative HDAC inhibitory drugs by uniting diverse features of *in silico* methodology. The molecular docking (XP dock), energetic based pharmacophore mapping, pharmacophore and atom based 3D QSAR model designing and study enables to establish activity correlation between structure of dataset molecules and its biological solicitation. It basically employs a combination of both structure and ligand based approaches. The ligand based pharmacophore was developed using Maestro v9.3. The dataset was selected from the earlier research findings. The target and ligand molecules were procured from recognized databases, which were incorporated into pivotal findings. The docking studies indicated the important intermolecular interactions between the moieties of ligands with the amino acids present in target protein. The developed 3D QSAR model expending the pharmacophore-based orientation exhibited extraordinary standards of regression coefficient for training set showing $Q^2 = 0.7753$ and $R^2 = 0.9834$ with low RMSD = 0.1085. The present findings would pave the way for design and development of novel HDAC inhibitors as anticancer agent.

Acknowledgements

Two of the authors, Harish Rajak and Preeti Patel are grateful to Science and Engineering Research Board – Department of Science & Technology (SERB-DST), New Delhi, India for providing financial assistance in the form of a Research project. One of the author, Vijay K. Patel is thankful to the Indian Council of Medical Research (ICMR), New Delhi for providing financial support in the form of Research Associate ship.

References

- Jiang Y, Yang Q & Zhang S, *Comp Chem*, 7 (2019) 51.
- Mohamed M F A, Shaykoon M S A & Abdel Rahman M H, *Bioorg Chem*, 72 (2017) 32.
- Wang G, Qiu J, Xiao X, Cao A & Zhou F, *Bioorg Chem*, 76 (2018) 249.
- Sun Q, Yao Y, Liu C, Li H, Yao H, Xue X, Liu J, Tu Z & Jiang S, *Bioorg Med Chem Lett*, 23 (2013) 3295.
- Yao Y, Liao C, Li Z, Wang Z, Sun Q, Liu C, Yang Y, Tu Z & Jiang S, *Eur J Med Chem*, 86 (2014) 639.
- Johnstone R W, *Nat Rev Drug Discov*, 1 (2002) 287.
- Ruijter A J D, Gennip A H V, Caron H N, Kemp S & Kuilenburg A B V, *Biochem J*, 370 (2003) 737.
- Bertrand P, *Eur J Med Chem*, 45 (2010) 2095.
- Yu C, He F, Qu Y, Zhang Q, Lv J, Zhang X, Xu A, Miao P & Wu J, *Bioorg Med Chem*, 26 (2018) 1859.
- Bisht N & Singh B K, *Int J PharmSci Res*, 9(4) (2018) 1405.
- Vijayakumar S, Manogar P, Prabhu S, Pugazhenthii M & Praseetha P K, *Comp Bio and Chem*, 78 (2019) 95.
- Patel P & Rajak H, *Med Chem Res*, 27 (2018) 2100.
- Patel P, Patel V K, Singh A, Jawaid T, Kamal M & Rajak H, *Curr Comp Aid Drug Des*, 14 (2018) 1.
- Patel V K, Chouhan K S, Singh A, Jain D K, Veerasamy R, Singour P K, Pawar R S & Rajak H, *Lett Drug Des Dis*, 12 (2015) 351.
- Jorgensen W L, Maxwell D S & Tirado-Rives J, *J Am Chem Soc*, 118 (1996) 11225.
- Kakarala K K, Jamil K & Devaraj V, *J Mol Graph Model*, 53 (2014) 179.
- Patel P, Patel V K, Singh A, Jawaid T, Mehnaz K & Rajak H, *Curr Comp Aid Drug Des*, 14 (2018) 1.
- Salam N K, Nuti R & Sherman W, *J Chem Inf Model*, 49 (2009) 2356.
- Watts K S, Dalal P, Murphy R B, Sherman W, Friesner R A & Shelley J C, *J Chem Inf Model*, 50 (2010) 534.
- Nair S B, Teli M K, Pradeep H & Rajanikant G K, *Comp Biol Med*, 42 (2012) 697.
- Teli M K & Rajanikant G K, *J Enzym Inhib Med Chem*, 27 (2012) 558.
- Dixon S L, Smondyrev A M, Knoll E H, Rao S N, Shaw D E & Friesner R A, *J Comput Aid Mol Des*, 19 (2006) 647.
- Golbraikh A & Tropsha A, *J Comput Aid Mol Des*, 16 (2002) 357.
- Patel P & Rajak H, *Med Chem Res*, 27 (2018) 2100.